Radboud Universiteit Nijmegen

The role of magnetism in phase transitions and pattern formation in iron and steel

Mikhail Katsnelson

IMM
Institute for Molecules and Materials

Epigraphs

To the theoretical physicists, ferromagnetism presents a number of very interesting, unsolved and beautiful challenges. Our challenge is to understand why it exists at all.

(Feynman Lectures on Physics)

Make things as simple as possible but not simpler

(A. Einstein)

Iron is special

^{56}Fe is the most stable nucleus, therefore there is a lot of iron (and nickel) in stars and planets

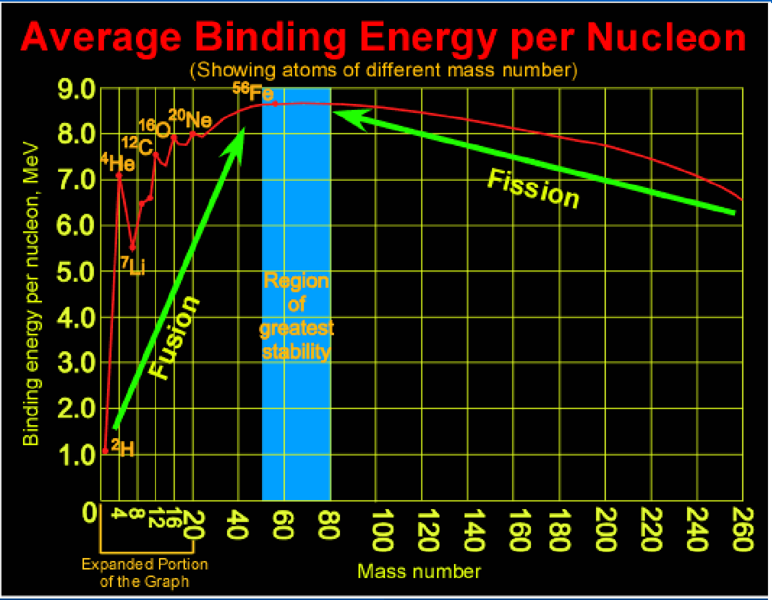

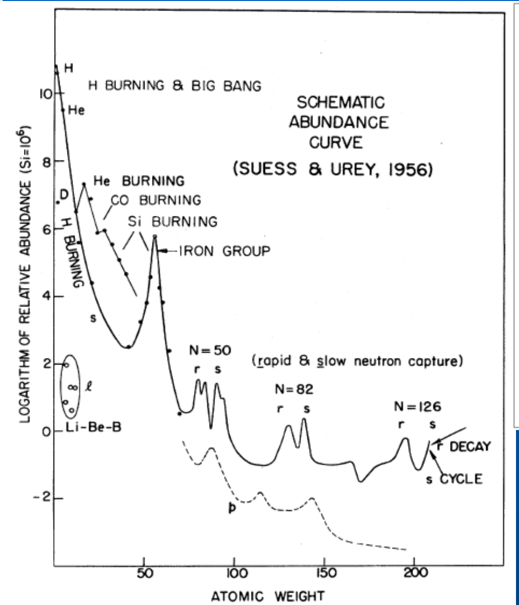

FIG. 2. Schematic curve of atomic abundances relative to $Si = 10^6$ vs atomic weight for the sun and similar main sequence stars.

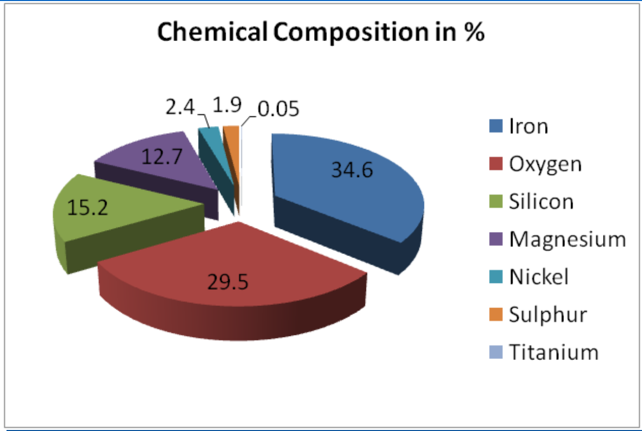

Chemical composition of Earth

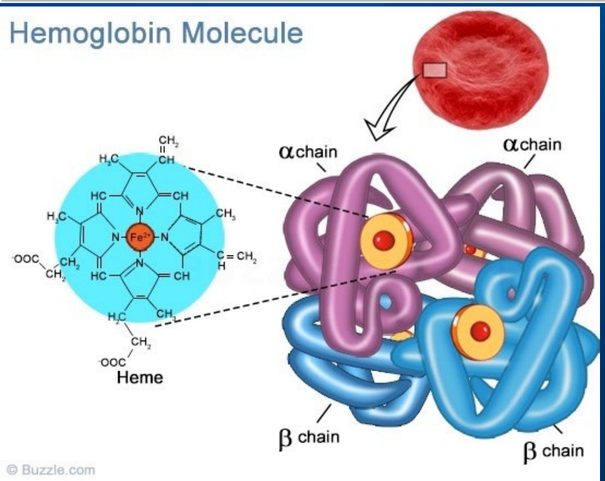

Crucially important for life (enzymes, oxygen trasfer, etc.)

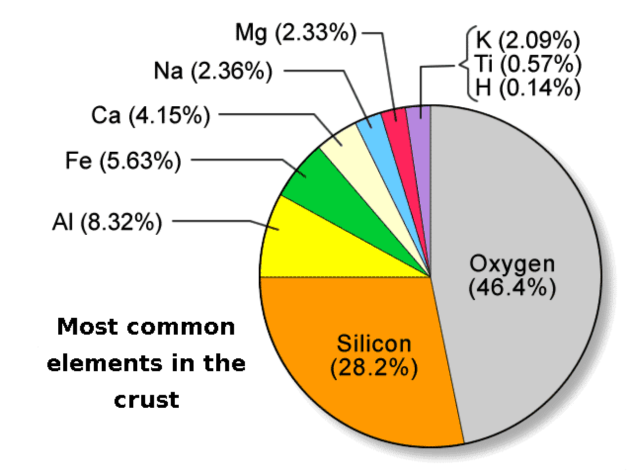

We are still in iron age

Steel (basically, Fe and a bit C) is one of the main materials of our civilization

Iron is polymorphous metal

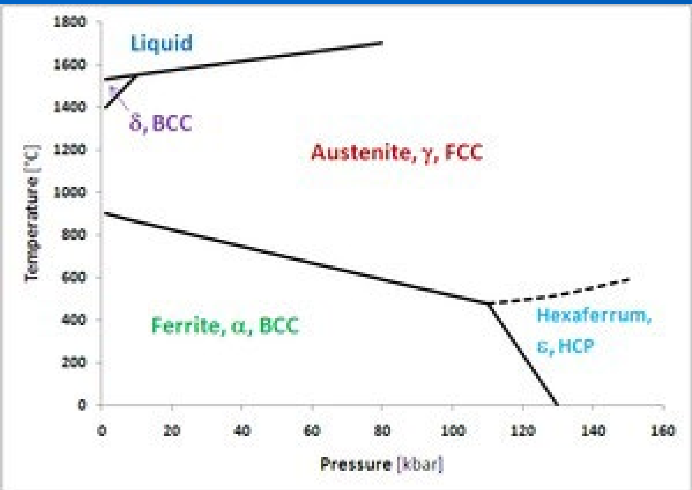

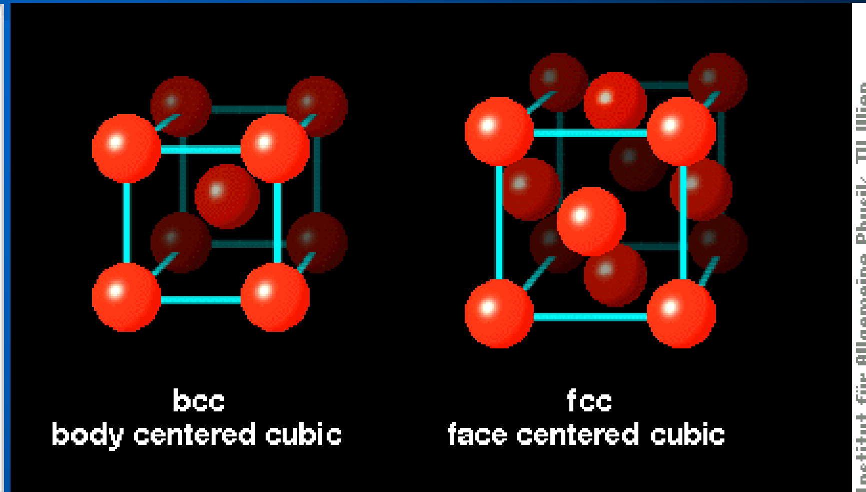

The only polymorphous metal where bcc phase is stable at lower temperatures than fcc or hcp: Role of magnetism (Zener)

Crucially important for Fe-C phase diagram and therefore for metallurgy

Should follow from electronic structure (quantum mechanical energy spectrum)

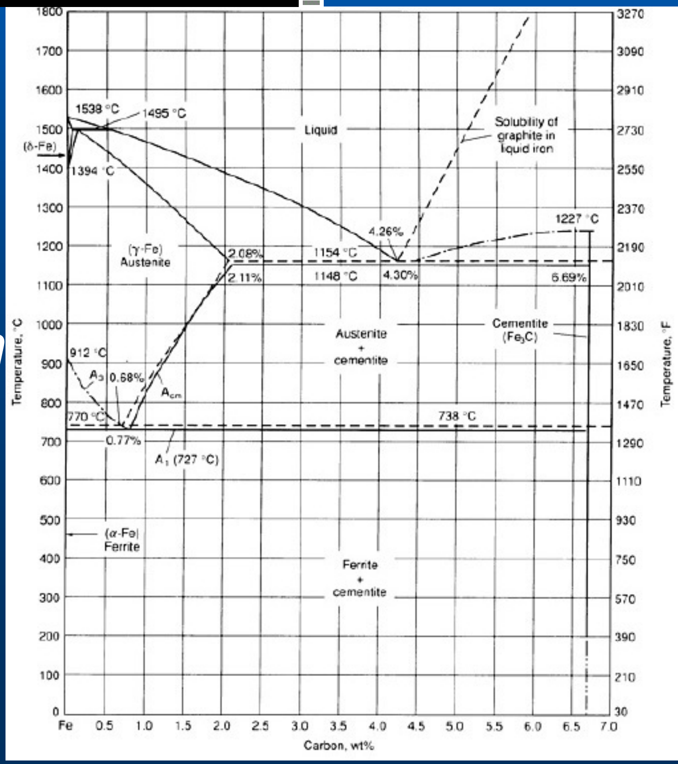

Long-standing problem

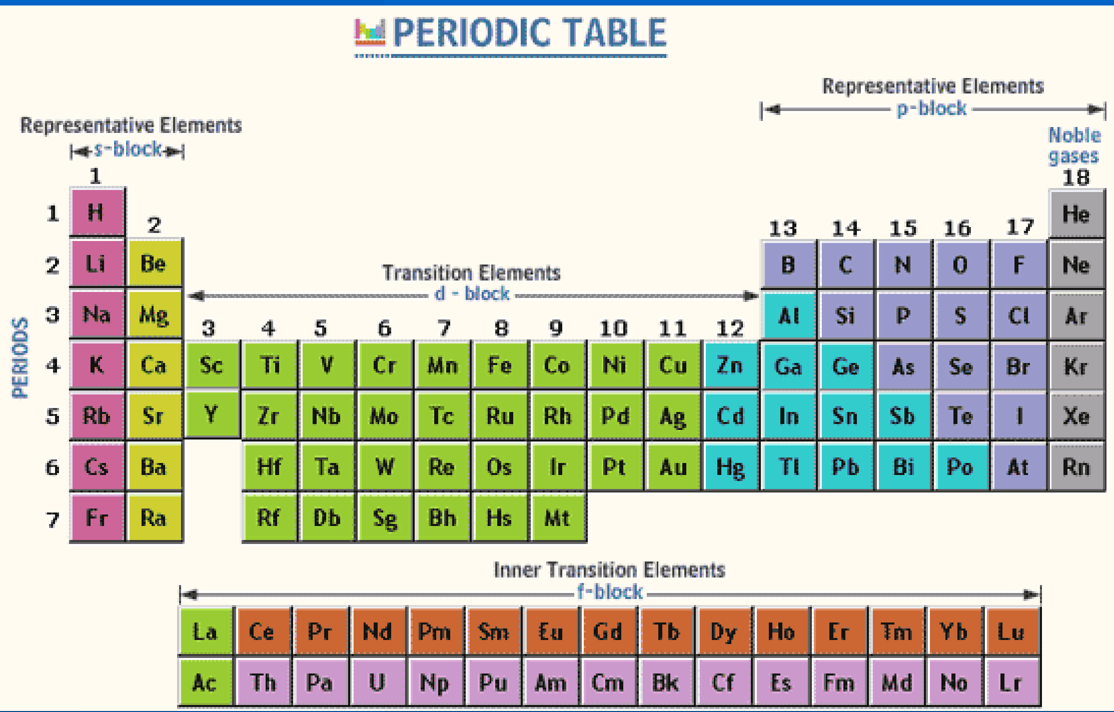

Ferromagnetism of iron
is known from ancient times

Iron

Cobalt

Nickel

Problem: coexistence of localized and itinerant behavior

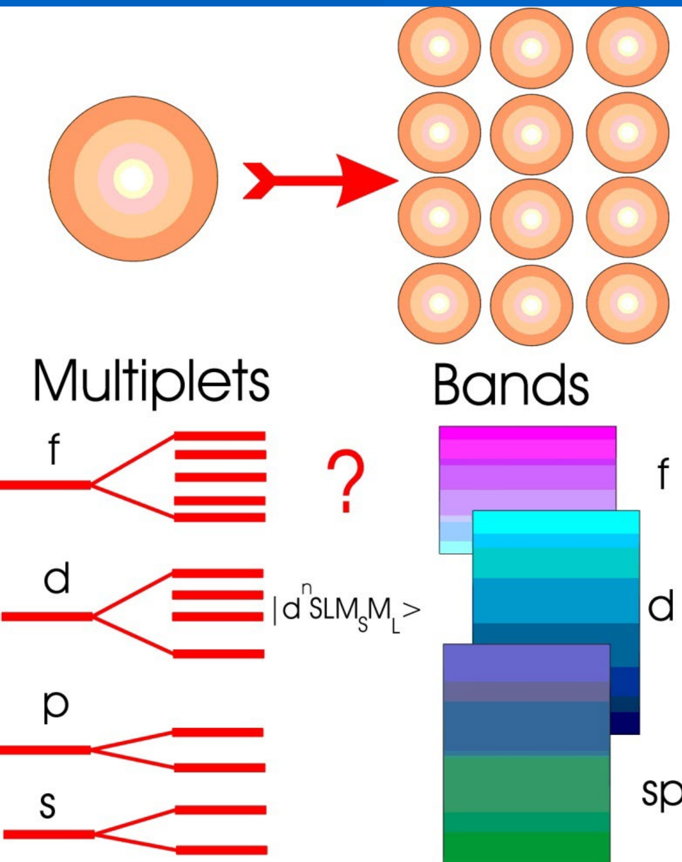

Local magnetic moments do exist above T_C (Curie-Weiss law, spectroscopy, neutrons…)

d electrons are itinerant (FS, chemical bonding, transport…)

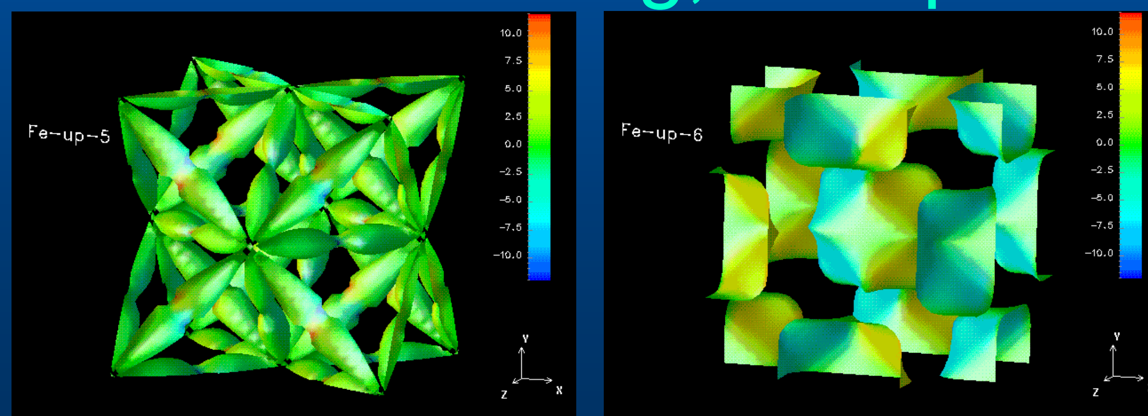

Iron, majority spin FS

4f electrons are normally pure localized but not 3d

Microscopic theory

Basis of our contemporary quantitative theory:
Density Functional Theory (DFT) + Dynamical Mean-Field Theory (DMFT) when necessary

Allows to calculate not only electronic structure and energetics, phonon spectra etc. but also magnetic interactions and magnetic phase diagrams

REVIEWS OF MODERN PHYSICS, VOLUME 95, JULY–SEPTEMBER 2023

Quantitative theory of magnetic interactions in solids

Attila Szilva and Yaroslav Kvashnin
Department of Physics and Astronomy, Division of Materials Theory, Uppsala University, Box 516, SE-75120 Uppsala, Sweden

Evgeny A. Stepanov
CPHT, CNRS, École polytechnique, Institut Polytechnique de Paris, 91120 Palaiseau, France

Lars Nordström
Department of Physics and Astronomy, Division of Materials Theory, Uppsala University, Box 516, SE-75120 Uppsala, Sweden and Wallenberg Initiative Materials Science for Sustainability, Uppsala University, 75121 Uppsala, Sweden

Olle Eriksson
Division of Materials Theory, Uppsala University, Box 516, SE-75120 Uppsala, Sweden and Wallenberg Initiative Materials Science for Sustainability, Uppsala University, 75121 Uppsala, Sweden

Alexander I. Lichtenstein
Institut für Theoretische Physik, Universität Hamburg, Notkestraße 9, 22607 Hamburg, Germany

Mikhail I. Katsnelson
Institute for Molecules and Materials, Radboud University, Heyendaalseweg 135, 6525 AJ Nijmegen, Netherlands

(published 11 September 2023)

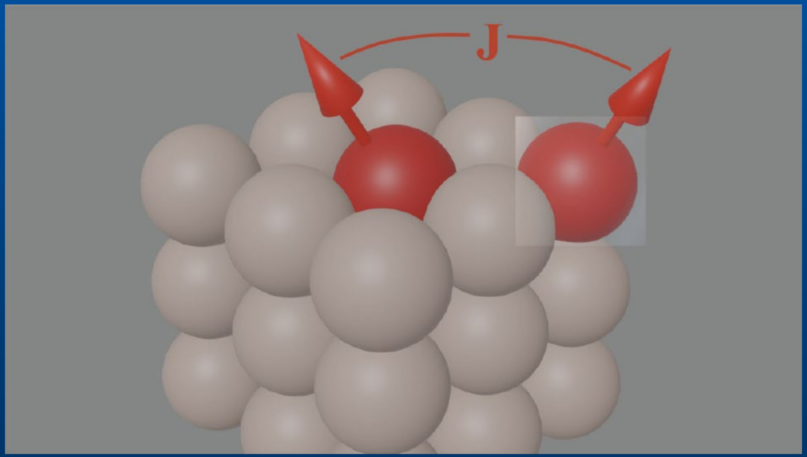

In this talk I will use mostly DFT results

Exchange interactions in bcc Fe

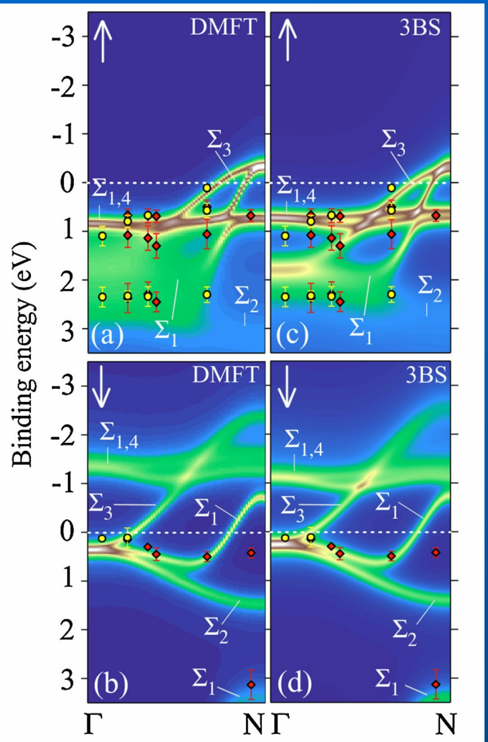

In electronic structure correlation effects beyond DFT are very essential (broadening, spectral density transfer…)

PRL 103, 267203 (2009) PHYSICAL REVIEW LETTERS week ending 31 DECEMBER 2009

Strength of Correlation Effects in the Electronic Structure of Iron

J. Sánchez-Barriga,[1] J. Fink,[1,2] V. Boni,[3] I. Di Marco,[4,5] J. Braun,[6] J. Minár,[6] A. Varykhalov,[1] O. Rader,[1] V. Bellini,[3] F. Manghi,[3] H. Ebert,[6] M. I. Katsnelson,[5] A. I. Lichtenstein,[7] O. Eriksson,[4] W. Eberhardt,[1] and H. A. Dürr[1]

Despite electronic structure is quite sensitive both exchange interactions and atomic forces are quite close (but not identical)

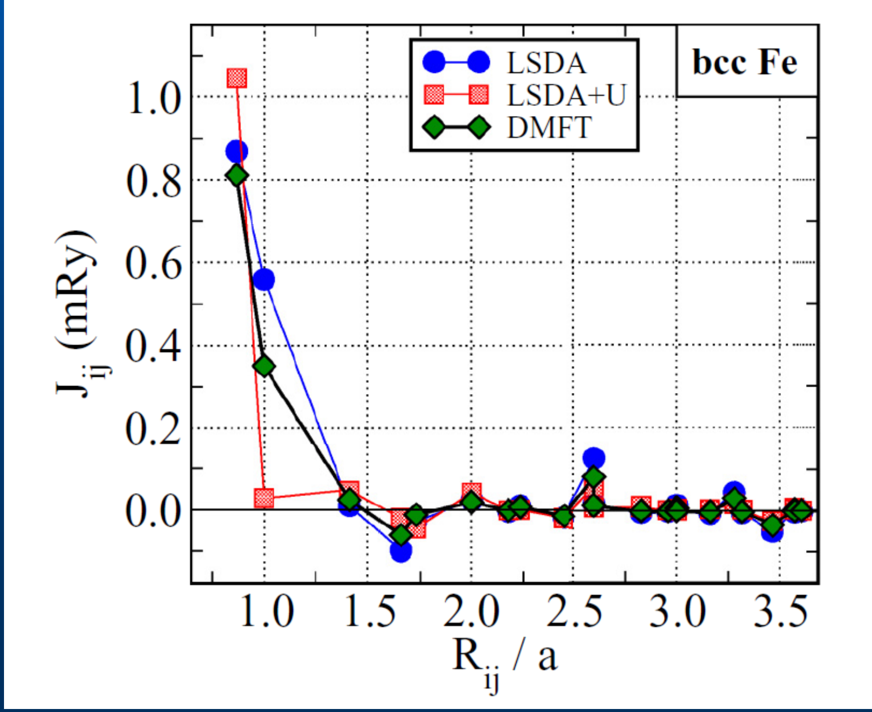

PHYSICAL REVIEW B 91, 125133 (2015)

Exchange parameters of strongly correlated materials: Extraction from spin-polarized density functional theory plus dynamical mean-field theory

Y. O. Kvashnin,[1] O. Grånäs,[1,2] I. Di Marco,[1] M. I. Katsnelson,[3,4] A. I. Lichtenstein,[4,5] and O. Eriksson[1]

Exchange interactions in bcc Fe II

Crucial role of e_g - t_{2g} splitting plus frustrations

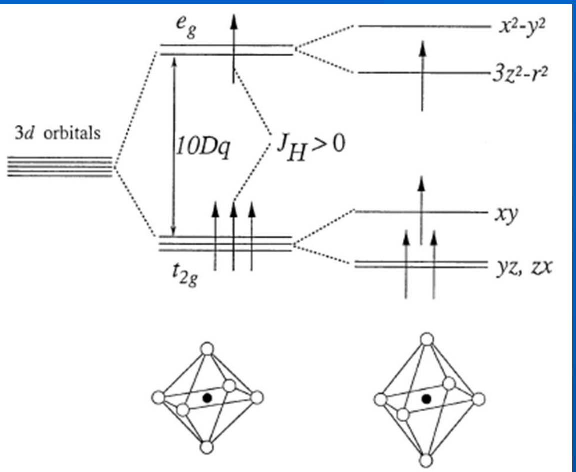

DOS in nonmagnetic bcc Fe

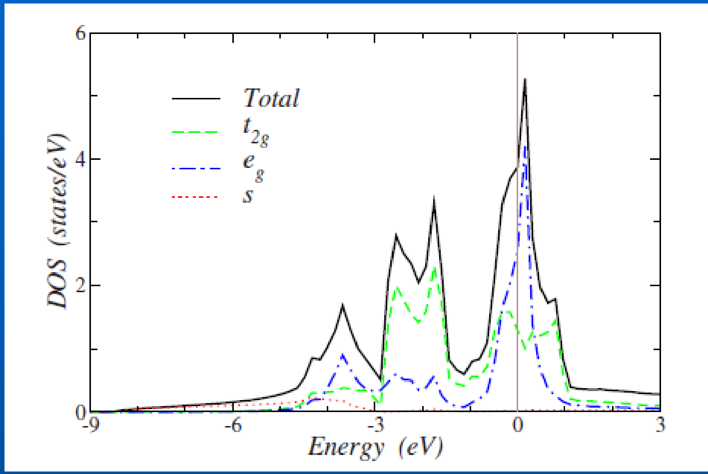

Stoner criterion is fulfilled due to e_g states only; they should play a special role in magnetism of Fe (Irkhin, Katsnelson, Trefilov, JPCM 5, 8763 (1993))

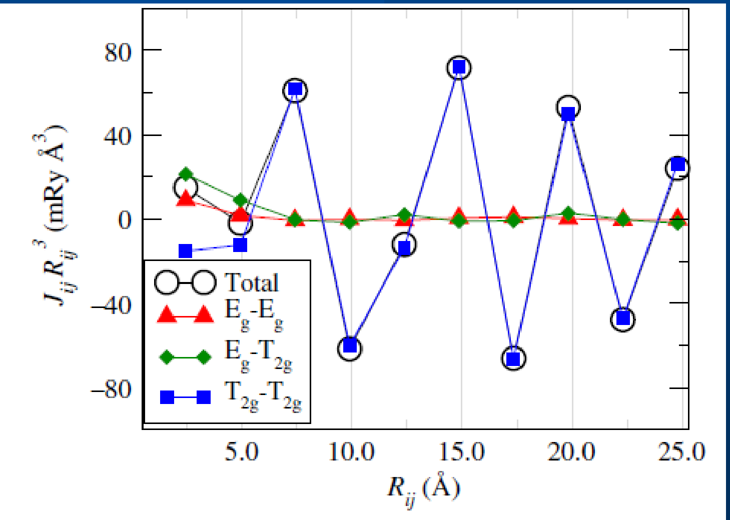

t_{2g} are itinerant electrons providing RKKY exchange with Friedel oscillations; e_g are more correlated providing (non-Heisenberg) "double exchange" typical for narrow-band systems

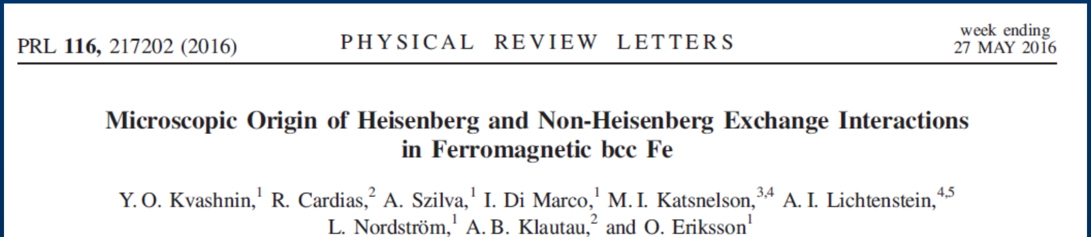
PRL **116**, 217202 (2016) PHYSICAL REVIEW LETTERS week ending 27 MAY 2016

Microscopic Origin of Heisenberg and Non-Heisenberg Exchange Interactions in Ferromagnetic bcc Fe

Y. O. Kvashnin,[1] R. Cardias,[2] A. Szilva,[1] I. Di Marco,[1] M. I. Katsnelson,[3,4] A. I. Lichtenstein,[4,5] L. Nordström,[1] A. B. Klautau,[2] and O. Eriksson[1]

Exchange interactions in fcc Fe

In fcc (γ) Fe very strong frustrations leading to noncollinear (e.g. spin spiral) structures

PHYSICAL REVIEW B **71**, 054402 (2005)

Origin of magnetic frustrations in Fe-Ni Invar alloys

A. V. Ruban,[1] M. I. Katsnelson,[2,3] W. Olovsson,[3] S. I. Simak,[3,4] and I. A. Abrikosov[4]

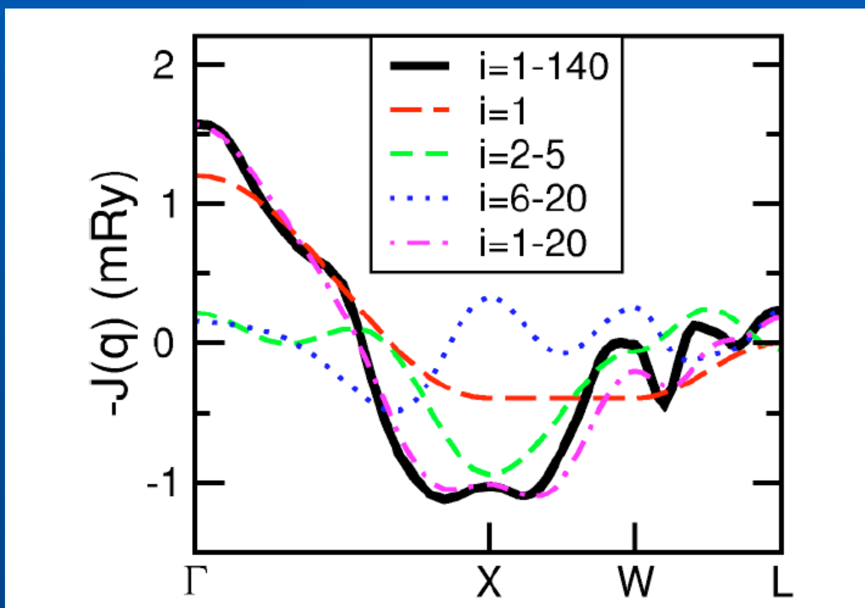

FIG. 2. (Color online) Energy of spin spiral in pure fcc Fe at atomic volume 77 a.u.[3] as a function of the spin-spiral wave vector **q**. The energy is estimated as $-J(\mathbf{q})$, and it is obtained from different sets of pair exchange parameters included in the Fourier-transform of J_{ij}, see text.

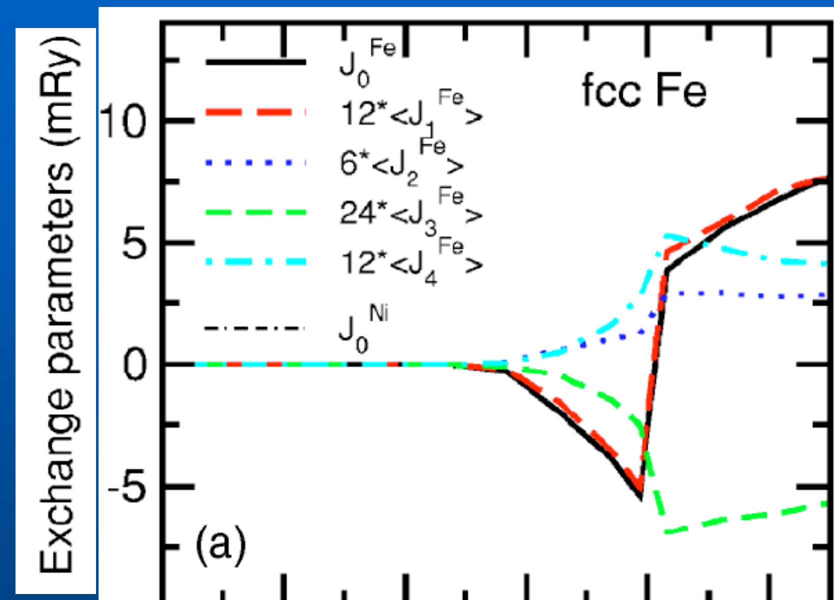

Contributions to the total exchange parameter from various coordination spheres

Exchange interactions in fcc Fe II

A very strong sensitivity of exchange parameters to lattice volume and shear deformations from fcc structure

Okatov, Gornostyrev, Lichtenstein & MIK, PR B 84, 214422 (2011)

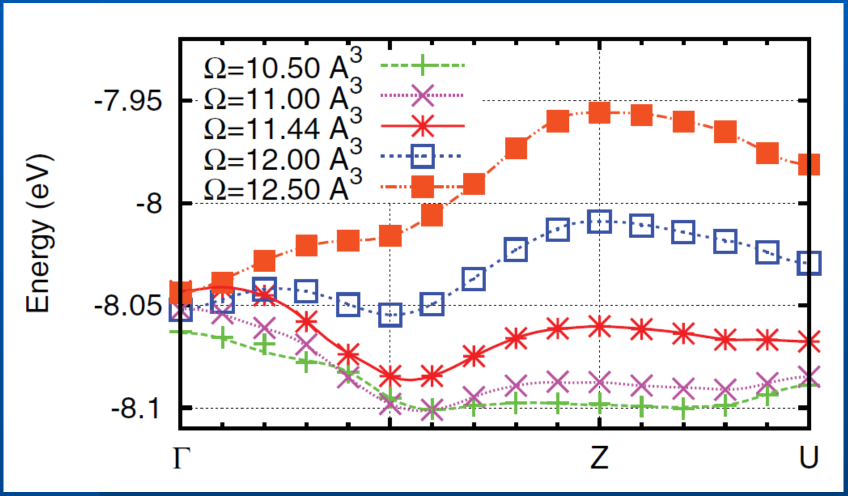

FIG. 2. (Color online) Dependence of the total energy of fcc Fe on the the spin spiral wave vector $E(\mathbf{Q})$ for different volumes (upper panel, $c/a = 1$) and for different c/a ratios (lower panel, $\Omega = 11.44$ Å^3). The deformations $c/a = 1/\sqrt{2}$ and $c/a = 1$ correspond to the bcc (α-Fe) and fcc (γ-Fe) structures, respectively. Symbols mark the results of the density-functional calculations whereas the lines correspond to Eq. (2) with obtained exchange parameters J_n.

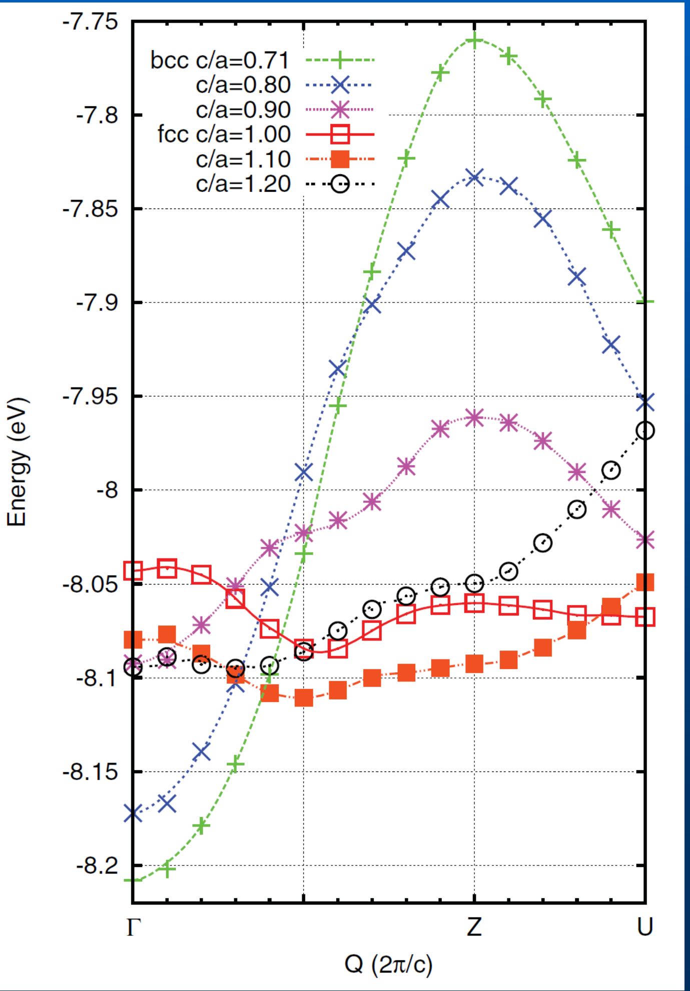

The effect of magnetism on lattice dynamics of Fe

The only polymorphous metal
where
bcc phase in not high-T is Fe

Why? Because usually bcc has soft phonon branches which increase entropy, and bcc gains. Without anharmonicities, it is typically even dynamically unstable

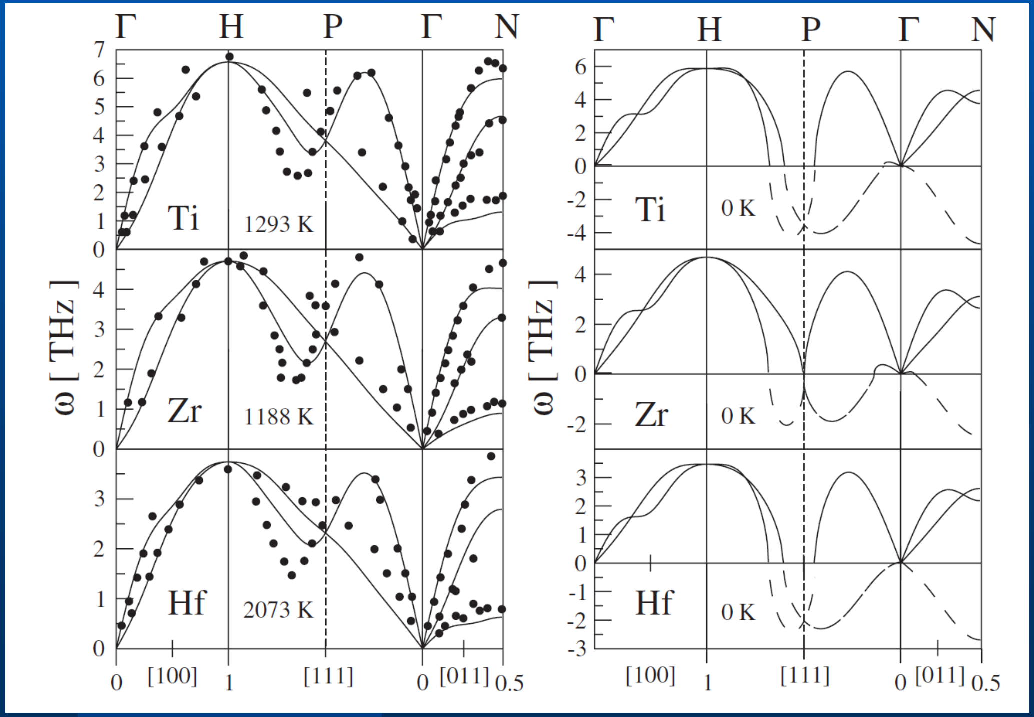

PRL 100, 095901 (2008) PHYSICAL REVIEW LETTERS week ending 7 MARCH 2008

Entropy Driven Stabilization of Energetically Unstable Crystal Structures Explained from First Principles Theory

P. Souvatzis,[1] O. Eriksson,[1] M. I. Katsnelson,[2] and S. P. Rudin[3]

Right column: harmonic (T = 0) calculations. Left: self-consistent phonon (anharmonic) calculations

The effect of magnetism of lattice dynamics II

Zener: bcc phase of Fe is stabilized by magnetism (DOS peaks destabilizing crystal lattice are moved from the Fermi energy)

Electronic correlations determine the phase stability of iron up to the melting temperature

SCIENTIFIC REPORTS | 4 : 5585

Published 7 July 2014

I. Leonov[1], A. I. Poteryaev[2,3], Yu. N. Gornostyrev[2,3], A. I. Lichtenstein[4], M. I. Katsnelson[5,6], V. I. Anisimov[2,6] & D. Vollhardt[1]

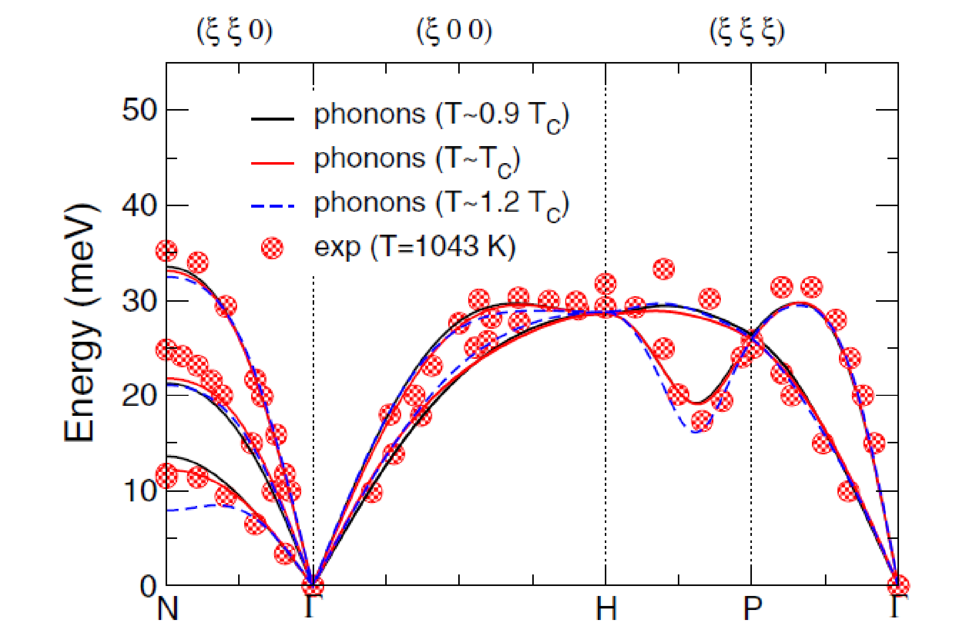

Figure 1 | Calculated phonon dispersion curves for bcc iron near the Curie temperature T_C. The results are compared with neutron inelastic scattering measurements at 1043 K.

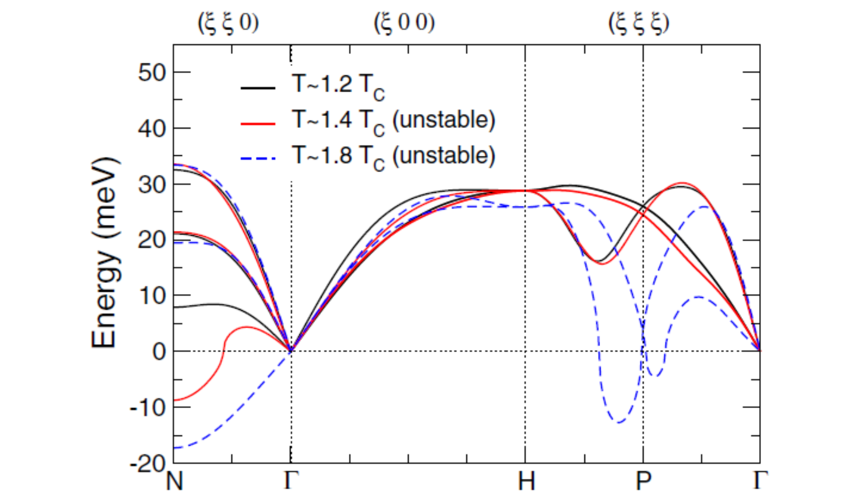

Figure 2 | Calculated phonon dispersions of paramagnetic bcc iron near the α-to-γ and γ-to-δ phase transitions for different temperatures.

Dynamical instability as a result of disappearance of magnetic moments

DMFT is essential!

α-γ transformation path

The simplest way to go continuously from bcc to fcc lattice is to represent fcc as bct with the ratio c/a=√2; two parameters: tetragonal deformation and volume (Bain distortion)

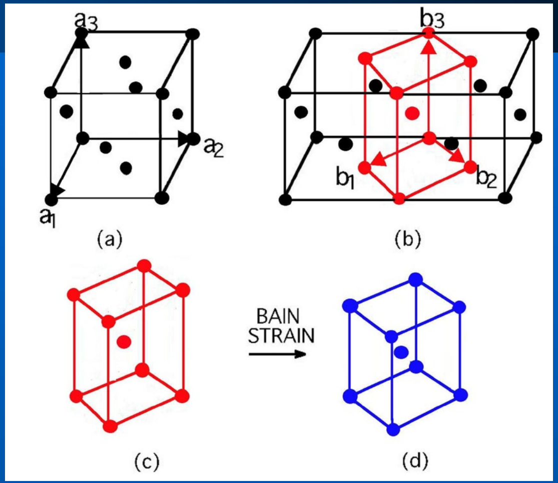

Okatov, Kuznetsov, Gornostyrev, Urtsev & MIK, PR B 79, 094011 (2011)

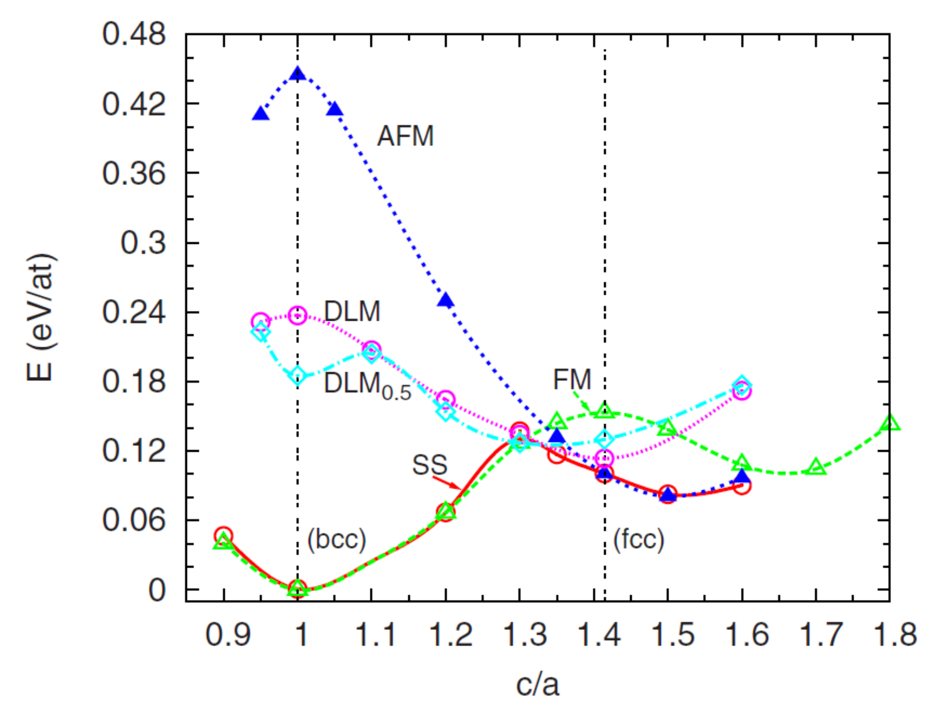

Energetics along Bain path for various magnetic states (FM, AFM, disordered moments, spin spirals)

Transition without barrier starting from FM state

Exchange interactions from α- to γ-Fe

Okatov, Gornostyrev, Lichtenstein & MIK, PR B 84, 214422 (2011)

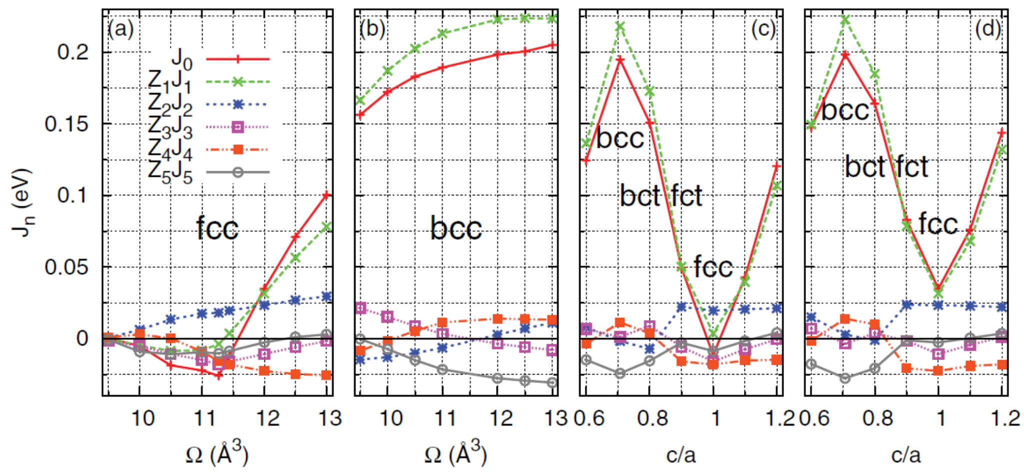

FIG. 3. (Color online) Exchange parameters J_n for $n = 1,2,3,4,5$ for different lattice parameters: dependence J_n on a volume of fcc (a) and bcc (b) Fe; dependence J_n on (c/a) at fixed volumes $\Omega = 11.44$ Å^3 (c) and $\Omega = 12.0$Å^3 (d), respectively.

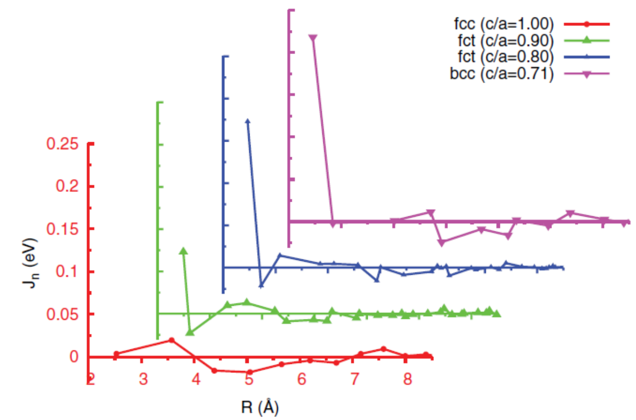

FIG. 5. (Color online) The exchange parameter as a function of interatomic distance to the nth neighbor $J_n(R_n)$ for different c/a ratios.

Exchange parameters are very sensitive not only to volume but also to tetragonal deformations – stabilization of fct phase

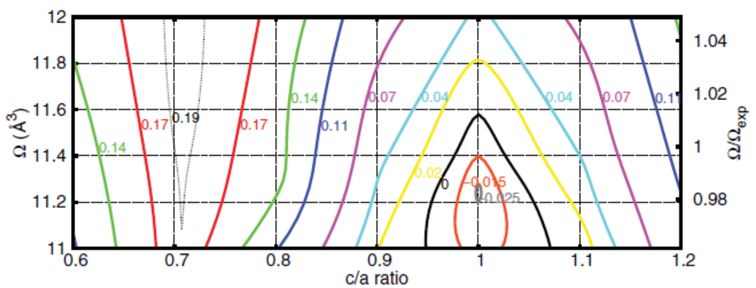

FIG. 4. (Color online) Dependence of the total exchange parameter J_0 on volume Ω and c/a ratio as a contour plot $J_0(\Omega, c/a)$.

Phase-field simulations: 2D model

J. Phys.: Condens. Matter 25 (2013) 135401 (9pp) doi:10.1088/0953-8984/25/13/135401

Effect of magnetism on kinetics of γ–α transformation and pattern formation in iron

I K Razumov[1,2], Yu N Gornostyrev[1,2] and M I Katsnelson[3]

PHYSICAL REVIEW B **90**, 094101 (2014)

Role of magnetic degrees of freedom in a scenario of phase transformations i

I. K. Razumov,[1,2,*] D. V. Boukhvalov,[3] M. V. Petrik,[2] V. N. Urtsev,[4] A. V. Shmakov,[4] M. I. Katsnelson,[5,6] and Yu. N. Gornostyrev[1,2]

Free-energy functional of deformations and magnetic state

$$G = \int \left(g_{\mathrm{e}} + \frac{k_{\mathrm{t}}}{2} (\nabla e_{\mathrm{t}})^2 \right) \mathrm{d}r,$$

$$g_{\mathrm{e}} = g_{\mathrm{t}}(e_{\mathrm{t}}, T) + \frac{A_{\mathrm{v}}}{2} e_{\mathrm{v}}^2 + \frac{A_{\mathrm{s}}}{2} e_{\mathrm{s}}^2,$$

$$e_v = (\varepsilon_{xx} + \varepsilon_{yy})/\sqrt{2} \qquad e_t = (\varepsilon_{xx} - \varepsilon_{yy})/\sqrt{2} \qquad e_s = \varepsilon_{xy}$$

$e_{\mathrm{t}} = 0$ in the γ-phase

$e_{\mathrm{t}} = 1 - 1/\sqrt{2}$ in the α-phase, i.e. $e_{\mathrm{t}} = (1 - c/a)$

$$A_v = C_{11} + C_{12}, \; A_s = 4C_{44}$$

Phase-field simulations: Magnetic part

$$E = E_{\mathrm{PM}}(\hat{\varepsilon}) - \sum_{i<j} J_{i,j}(\hat{\varepsilon}) Q_{ij}(T)$$

$$Q_{ij}(T) \equiv \langle \mathbf{m}_i \cdot \mathbf{m}_j \rangle$$

To simplify: nearest-neighbor approximation for J

$$g(\hat{\varepsilon}, T) = g_{\mathrm{PM}}(\hat{\varepsilon}) - \tilde{J}(\hat{\varepsilon}) \tilde{Q}(T)$$

$$\tilde{J}(\hat{\varepsilon}) = g_{\mathrm{PM}}(\hat{\varepsilon}) - g_{\mathrm{FM}}(\hat{\varepsilon})$$

$$\tilde{Q}(T) \equiv \frac{\langle \mathbf{m}_0 \cdot \mathbf{m}_1 \rangle}{m^2} = \frac{1 + \exp(-kT_{\mathrm{C}}/\lambda)}{1 + \exp(k(T - T_{\mathrm{C}})/\lambda)}$$

Parameters are taken to fit experimental Curie temperature of α-Fe (1043 K) and

$$Q(T_C) \sim 0.4$$

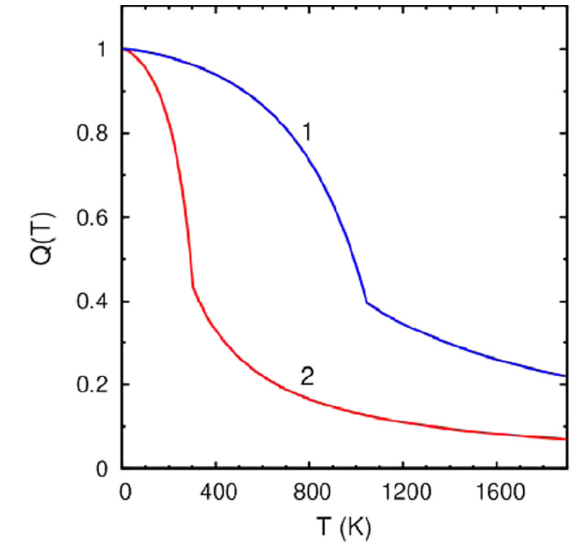

FIG. 1. (Color online) Temperature dependencies of the spin correlator $Q(T)$ for α-Fe (1) and γ-Fe (2).

Phase-field simulations: Kinetic equations

$$\rho \frac{\partial^2 u_i(\mathbf{r},t)}{\partial t^2} = \sum_j \frac{\partial \sigma_{ij}(\mathbf{r},t)}{\partial r_j}$$

$$\sigma_{ij}(\mathbf{r},t) = \frac{\delta F}{\delta \varepsilon_{ij}(\mathbf{r},t)}$$

$$\phi = \sqrt{2}/(\sqrt{2}-1)e_t, \quad e_v = (\varepsilon_{xx} + \varepsilon_{yy})/\sqrt{2},$$
$$e_t = (\varepsilon_{xx} - \varepsilon_{yy})/\sqrt{2},$$

$$\varepsilon_{xx} = \frac{\partial u_x}{\partial x}, \qquad \varepsilon_{yy} = \frac{\partial u_y}{\partial y}, \qquad \varepsilon_{xy} = \frac{1}{2}\left(\frac{\partial u_x}{\partial y} + \frac{\partial u_y}{\partial x}\right)$$

$$\sigma_{xx} = \frac{1}{(\sqrt{2}-1)} \frac{df(c,\phi,T)}{d\phi} + \tilde{A}_v e_v - \tilde{k}_t \nabla^2 \phi,$$

$$\sigma_{yy} = -\frac{1}{(\sqrt{2}-1)} \frac{df(c,\phi,T)}{d\phi} + \tilde{A}_v e_v + \tilde{k}_t \nabla^2 \phi,$$

$$\sigma_{xy} = A_s e_s,$$

Phase field simulations: Results

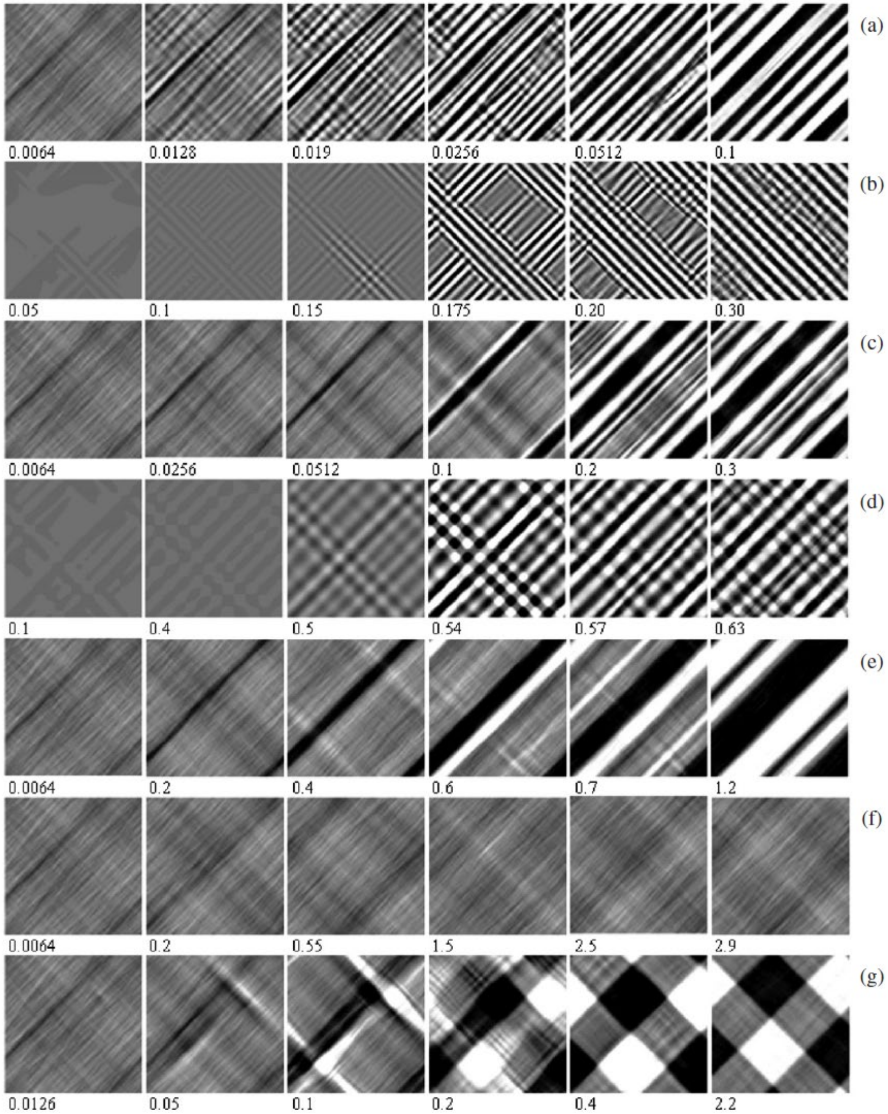

Figure 2. Time evolution of the structure at exposure at $T = 400$ K ((a), (b)), 700 K ((c), (d)), 950 K (e), 1000 K ((f), (g)) after quenching of the high-temperature state ((a), (c), (e), (f)) or development of instability of the uniform fcc state ((b), (d)), under homogeneous ((a)–(f)) and heterogeneous nucleation (g). Gradations of gray color correspond to the values for the order parameter ϕ; black and white colors show the regions for the α-phase with two possible orientations ($\phi = \pm 1$).

$$\phi = \sqrt{2}/(\sqrt{2}-1)e_t$$

normalized parameter of Bain deformation

$$-1 < \phi < 1$$

Magnetic free energy plays crucial role in kinetics of transformation and morphology of the final structure in pure iron

Carbon impurity in γ-Fe: Role of exchange interactions

PRL **99,** 247205 (2007) PHYSICAL REVIEW LETTERS week ending 14 DECEMBER 2007

Magnetism and Local Distortions near Carbon Impurity in γ-Iron

D. W. Boukhvalov
Institute for Molecules and Materials, Radboud University Nijmegen, NL-6525 ED Nijmegen, the Netherlands
Institute of Metal Physics, Russian Academy of Sciences, Ural Division, Ekaterinburg 620041, Russia

Yu. N. Gornostyrev
Institute of Metal Physics, Russian Academy of Sciences, Ural Division, Ekaterinburg 620041, Russia
Institute of Quantum Materials Science, Ekaterinburg 620107, Russia

M. I. Katsnelson
Institute for Molecules and Materials, Radboud University Nijmegen, NL-6525 ED Nijmegen, the Netherlands

A. I. Lichtenstein
Institut für Theoretische Physik, Universität Hamburg, 20355 Hamburg, Germany
(Received 25 June 2007; published 13 December 2007)

Long-standing problem: solution enthalpy of C in γ-Fe

Solution: local tetragonal distortions and local FM ordering

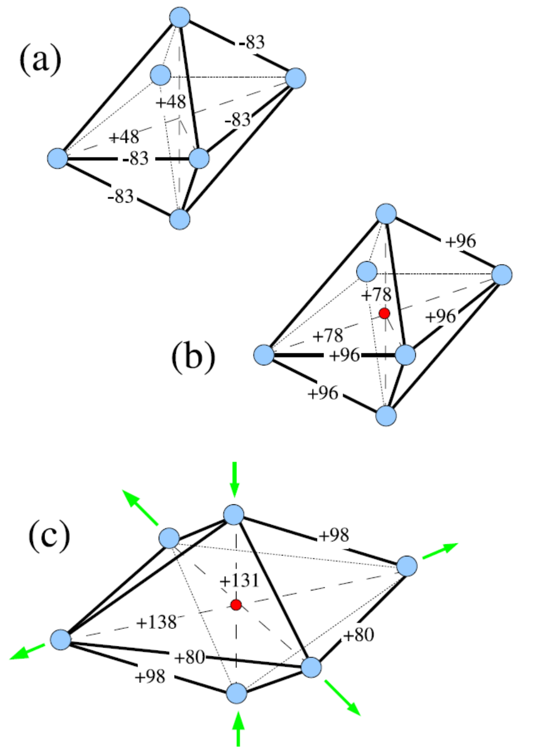

FIG. 2 (color online). Exchange parameters (in K) for different Fe-Fe pairs in original fcc lattice (a); in fcc lattice with carbon interstitial impurity without (b) and with (c) relaxation taken into account. Arrows indicate direction of atomic displacements during the relaxation.

Solution enthalpy 0.55 eV (exp. 0.4 eV)

Deformations make C-C interaction much stronger (not pure dilatation centers)

Steel as composite material

Carbon does not like to be neither in α or in γ phase, it likes to sit in carbides (cementite Fe_3C)

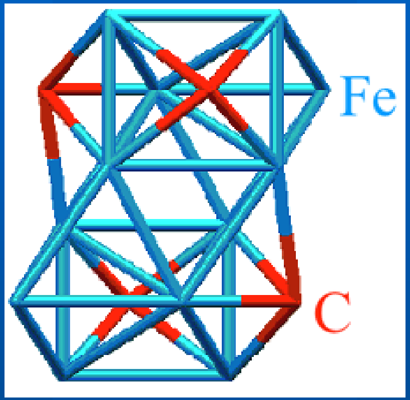

Morphology of two-phase state (ferrite, that is α-phase, and cementite) determines mechanical properties

Originates from the cooling of high-temperature γ-phase

Kinetics is crucial. Two limit cases:

- *Ferrite transformation (the slowest one carbon has a time to diffuse)*
- *Martensitic transformation (very fast, carbon is captured where it was)*

Phase-field simulations for steel

PHYSICAL REVIEW B **90**, 094101 (2014)

Role of magnetic degrees of freedom in a scenario of phase transformations in steel

I. K. Razumov,[1,2,*] D. V. Boukhvalov,[3] M. V. Petrik,[2] V. N. Urtsev,[4] A. V. Shmakov,[4]
M. I. Katsnelson,[5,6] and Yu. N. Gornostyrev[1,2]

Adding carbon concentration c as parameter

$$F = \int \left(f(c, e_t, T) + \frac{A_v}{2} e_v^2 + \frac{A_s}{2} e_s^2 + \frac{k_t}{2} (\nabla e_t)^2 \right) dr$$

Adding entropy contribution

$$\begin{aligned} f(c, e_t, T) = {} & g_{\mathrm{PM}} - T s_0 f_s(e_t) \\ & - \int_0^{\tilde{J}} Q(\tilde{J}', T) d\tilde{J}' + kT \left\{ c \ln(4c) \right. \\ & \left. + \left[c \ln \frac{c}{3} - c \ln(4c) \right] [1 - f_s(e_t)] \right\} \end{aligned}$$

Parametrizing dependence on deformation along Bain path

$$\begin{aligned} \tilde{g}_{\mathrm{PM(FM)}}(\phi) = {} & g^{\mathrm{fcc}}_{\mathrm{PM(FM)}} \\ & + 2 \left(g^{\mathrm{bcc}}_{\mathrm{PM(FM)}} - g^{\mathrm{fcc}}_{\mathrm{PM(FM)}} + \frac{c_{\mathrm{PM(FM)}}}{6} \right) \\ & \times \left(\phi^2 - \frac{\phi^4}{2} \right) + c_{\mathrm{PM(FM)}} \left(\frac{\phi^6}{3} - \frac{\phi^4}{2} \right) \end{aligned}$$

Phase-field simulations for steel II

Adding diffusion to EOM

$$\rho \frac{\partial^2 u_i(\mathbf{r},t)}{\partial t^2} = \sum_j \frac{\partial \sigma_{ij}(\mathbf{r},t)}{\partial r_j}$$

$$\frac{\partial c}{\partial t} = -\nabla \mathbf{I}.$$

$$\sigma_{ij}(\mathbf{r},t) = \frac{\delta F}{\delta \varepsilon_{ij}(\mathbf{r},t)}, \quad \mathbf{I} = -\frac{D}{kT} c(1-c)\nabla\left(\frac{\delta F}{\delta c}\right)$$

Diffusion parameters were taken from experiment

Phase-field simulations for steel III

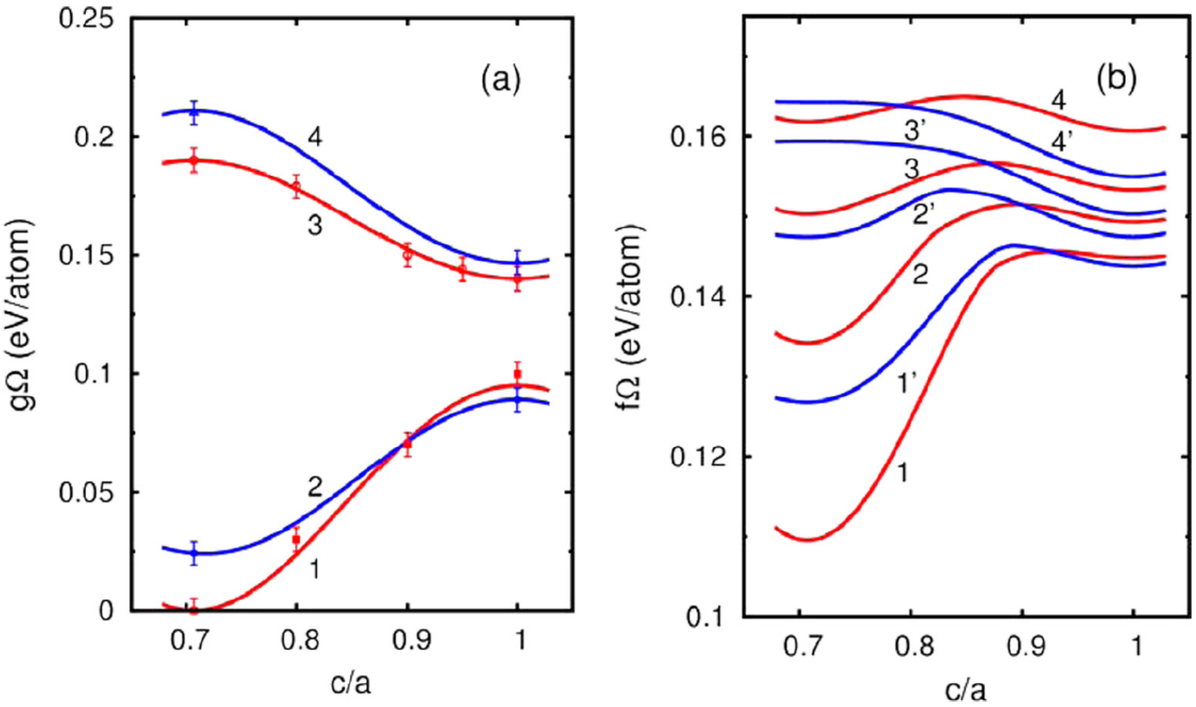

FIG. 2. (Color online) Energy (a) resulting from the first-principles calculation for the Bain path in ferromagnetic (curves 1,2) and paramagnetic (3,4) states for carbon concentration $C = 0$ (1,3) and $C = 3$ at. % (2,4). Free energy (b) as functions of tetragonal deformation for temperatures $T = 600$ K (curves $1, 1'$), 800 K ($2, 2'$), 1000 K ($3, 3'$), and 1400 K ($4, 4'$) found from Eq. (5) and the first-principles computational results for carbon concentration $C = 0$ and $C = 3$ at. %, respectively. Symbols correspond to the computational results; solid lines are approximations used in the model.

Phase-field simulations for steel IV

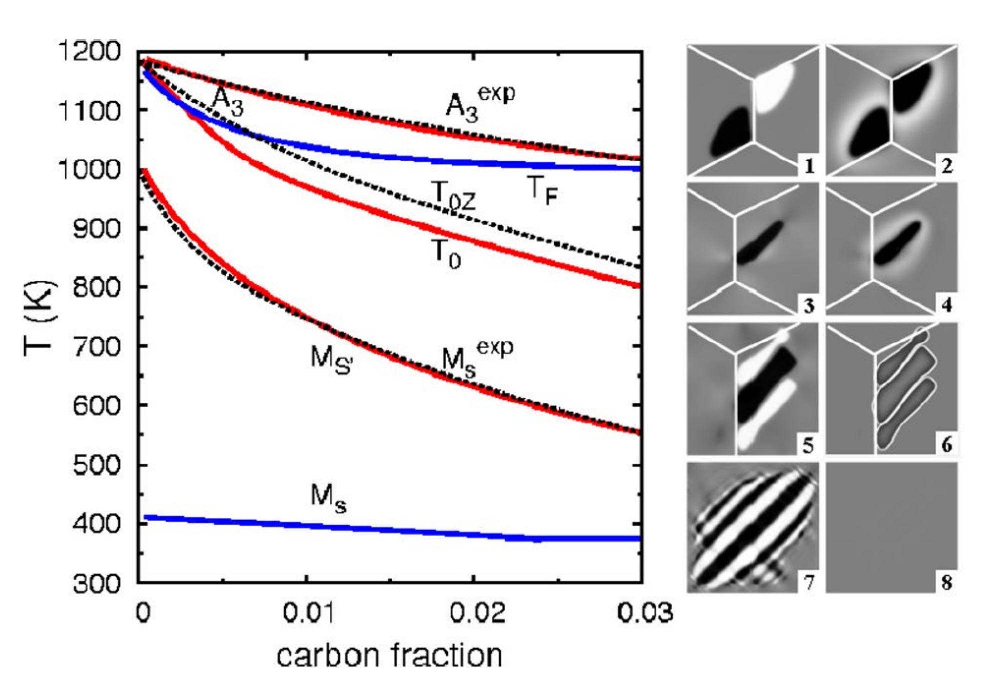

FIG. 4. (Color online) The left panel shows calculated lines (solid) corresponding to the start of ferrite transformation, paraequilibrium, and the start of martensitic transformation. M_s and $M_{s'}$ are the temperatures at the start of lattice instability and martensitic-like transformation. Dashed lines show the experimental boundary of the two-phase region (A_3) [36], the experimental paraequilibrium temperature (T_{0Z}) [37], and the experimental temperature of the start of martensitic transformation ($M_s^{\text{expt.}}$) [35]. The right panel shows microstructures forming as a result of transformation at various temperatures: $T_0 < T < A_3$ (1,2), $M_{s'} < T < T_0$ (3,4; 5,6), and $T < M_{s'}$ (7,8). The left and right columns in this panel correspond to tetragonal strain (black and white are two orthogonal directions of tetragonal deformation in bcc phase; gray shows fcc regions) and carbon distribution (the darker the smaller), respectively.

Pearlite structure

A special morphology very favorable for mechanical properties; A long-standing problem to explain

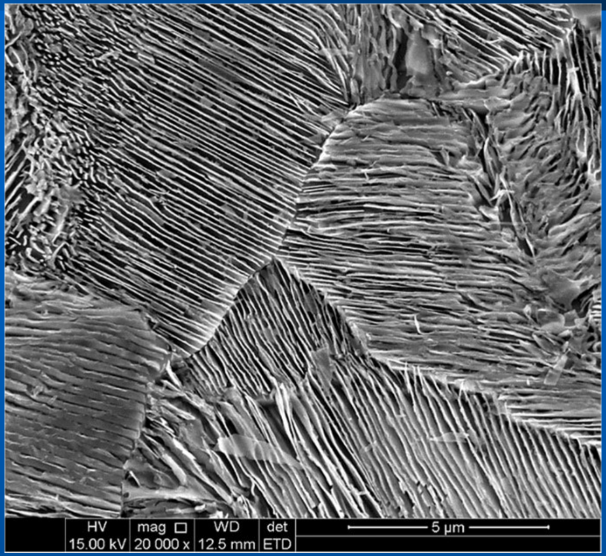

Pearlitic structure in rail steel (Sci Rep 9, 7454 (2019))

A very useful language to unify description of α-, γ- and θ- phases (orthorombic phase of cementite)

Structural transformations among austenite, ferrite and cementite in Fe–C alloys: A unified theory based on *ab initio* simulations

Xie Zhang [a,*], Tilmann Hickel [a], Jutta Rogal [b], Sebastian Fähler [c,d], Ralf Drautz [b], Jörg Neugebauer [a]

Acta Materialia 99 (2015) 281–289

metastable intermediate structure (MIS), which can serve as a link between the three phases

Feromagnetism and tetragonal distortions in γ-Fe

Long-known fact: FM fcc Fe is unstable with respect to the tetragonal distortion (c/a>1)

PHYSICAL REVIEW B VOLUME 60, NUMBER 1 1 JULY 1999-I

Tetragonal equilibrium states of iron

P. M. Marcus and V. L. Moruzzi
IBM Research Division, T.J. Watson Research Center, Yorktown Heights, New York 10598

S.-L. Qiu
Department of Physics, Alloy Research Center, Florida Atlantic University, Boca Raton, Florida 33431-0991
(Received 6 January 1999)

First-principles total-energy calculations on tetragonal Fe show that the ferromagnetic and antiferromagnetic phases have tetragonal equilibrium states with $c/a>1$, the fcc value. The bulk layers of an epitaxial film of Fe on Cu(001), which are almost fcc with the Cu lattice constant, are shown to be stable in the antiferromagnetic phase, but inherently unstable in the ferromagnetic phase. The structure of tetragonal equilibrium antiferromagnetic Fe is estimated to be $a=3.47$ Å, $c=3.75$ Å. [S0163-1829(99)04125-9]

From Zhang et al paper:

Within the FM-HS state, fcc Fe is unstable and can directly relax to a face-centered tetragonal (fct) state with $c/a = 1.17$. Hence, the initial geometry of austenite is treated as fct in the FM-HS state.

Feromagnetism and tetragonal distortions in γ-Fe II

This tetragonal distortion is a prerequisite of θ-phase: just add carbon

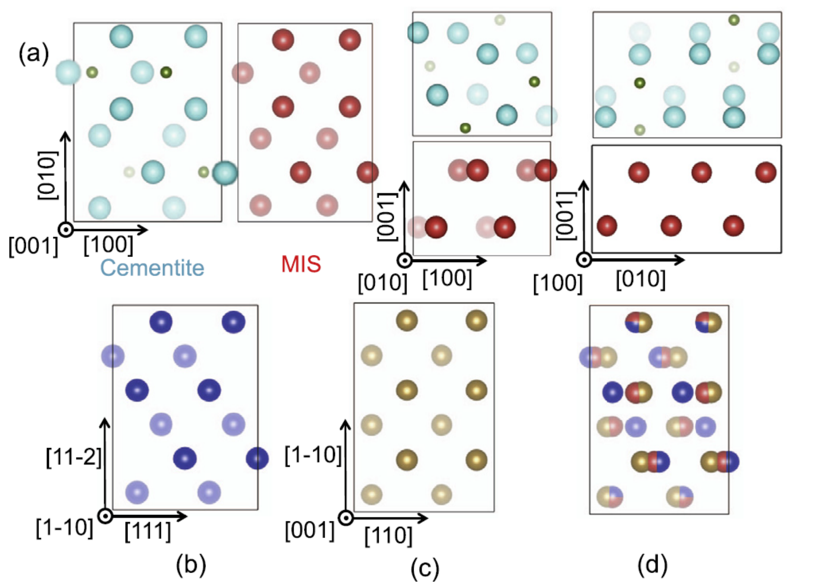

Fig. 1. (a) shows the comparison between cementite and the MIS in three projections. Large spheres represent Fe atoms and small green spheres refer to C. In the second row the orthorhombic unit cells of ferrite (b) and austenite (c) are shown. In (d) a comparison of the atomic positions of the MIS, ferrite and austenite is shown. Lower-lying atoms are shaded with gray color. The structures in this paper are visualized with the VESTA program [36]. (For interpretation of the references to color in this figure caption, the reader is referred to the web version of this article.)

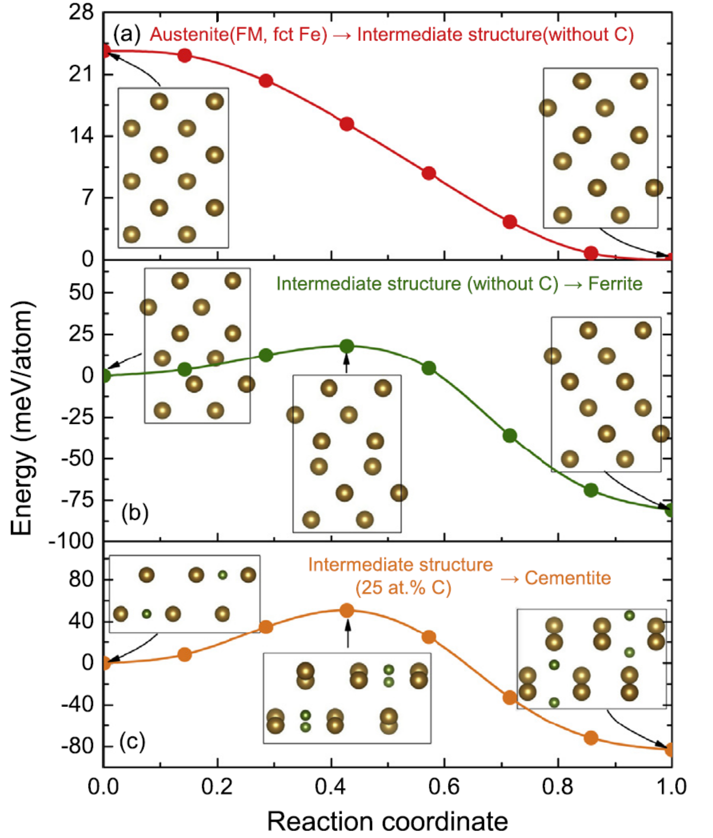

X. Zhang et al. / Acta Materialia 99 (2015) 281–289

Autocatacytic mechanism of pearlite transformation

PHYSICAL REVIEW APPLIED **7,** 014002 (2017)

Autocatalytic Mechanism of Pearlite Transformation in Steel

I. K. Razumov,[1,2,*] Yu. N. Gornostyrev,[1,2,4] and M. I. Katsnelson[3,4]

Scenario

- At high temperature, α-phase is still FM and it can iduce FM in neighboring γ-phase
- This induces FM leads to tetragonal deformation in γ-phase which makes it very close to MIS preparing positions for carbon
- Carbon easily diffuse there forming θ-phase

Magnetism seems to be crucially important!

Autocatacytic mechanism of pearlite transformation II

Phase-field simulations unifying three phases

$$F = \int \left(f_{\text{eff}}(c, T) + \frac{k_c}{2} (\nabla c)^2 \right) d\mathbf{r}$$

$$f_{\text{eff}}(c, T) = \min\{ f_\alpha(c, T), f_\gamma(c, T), f_\theta(c, T) \}$$

$$\frac{\partial c}{\partial t} = -\nabla \mathbf{I}, \qquad \mathbf{I} = -\frac{D(c)}{kT} c(1 - c) \nabla \left(\frac{\delta F}{\delta c} \right)$$

$$D(c) = [D_\gamma + (D_\alpha - D_\gamma) h(C_{T0} - c)] h(C_{T1} - c) + D_\theta h(c - C_{T1}),$$

$h(x)$ is a smoothed Heaviside step function

Phase field results

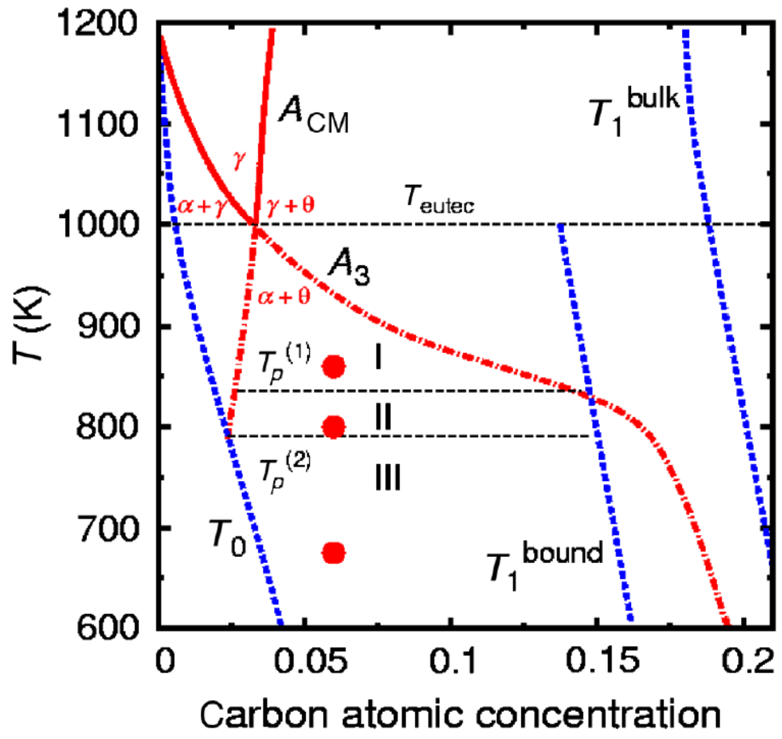

FIG. 2. The calculated transformation diagram. The lines A_3 and A_{CM} are the boundaries of two-phase regions $\alpha + \gamma$ and $\gamma + \theta$ as well as their metastable extensions below the eutectoid temperature T_{eutec}; the lines T_0 and T_1 are lines of instability with respect to the $\gamma \to \alpha$ and $\gamma \to \theta$ transformations, respectively. The temperature regions I–III are determined by the intersection points of these lines. The circles indicate the conditions under which the simulations are carried out.

Phase field results II

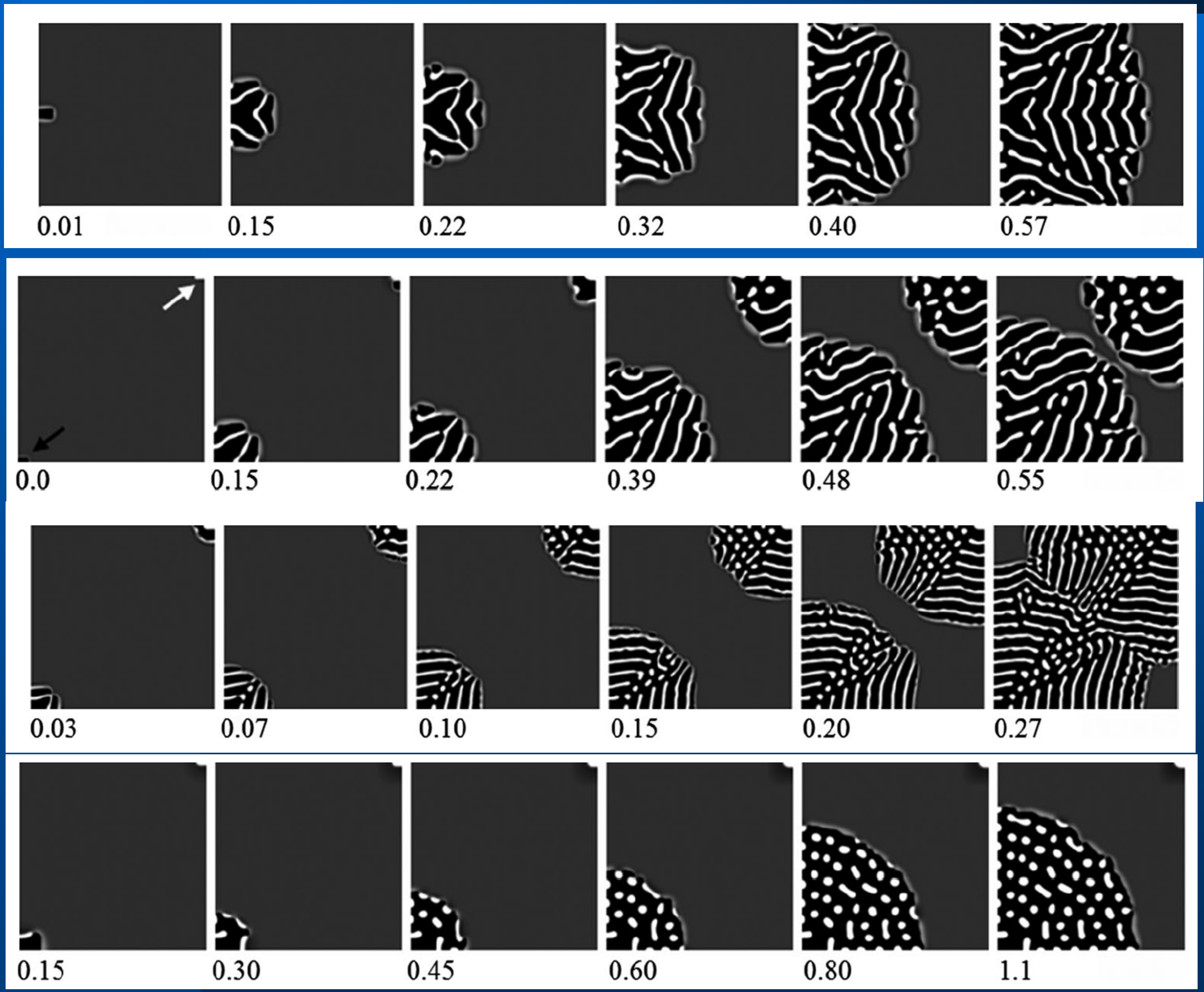

Conclusions

Magnetism of Fe is crucially important for metallurgy, and correlation effects are important for magnetism

Better understanding of metallurgical processes requires quantum many-body theory

Many thanks to many collaborators, especially Yuri Gornostyrev